**Janusz Fabia,
Jarosław Janicki,
Czesław Ślusarczyk,
Monika Rom,
Tadeusz Graczyk,
Andrzej Gawłowski**

**University of Bielsko-Biala,
Institute of Textile Engineering
and Polymer Materials,**
ul. Willowa 2, 43-309 Bielsko-Biala, Poland;
E-mail: jfabia@ath.bielsko.pl

Study of Structure of Polypropylene Microfibres Modified with Multi-Walled Carbon Nanotubes

Abstract
The paper presented is concerned with studies of a supermolecular structure and its transformation during the process of drawing new composite microfibres obtained from isotactic polypropylene (iPP) – as a matrix and multi-walled carbon nanotubes (MWCNT) used as the filler. The nanostructure of iPP/MWCNT microfibres as spun and after drawing at a temperature of 95°C was investigated using scanning electron microscopy (SEM), wide angle X-ray scattering (WAXS), small angle X-ray scattering (SAXS) and differential scanning calorimetry (DSC) methods.

Key words: *polypropylene microfibres, multi-walled carbon nanotubes, modification, structure.*

Introduction

Polypropylene (iPP) fibres are the third, after polyester and polyamide, most important synthetic fibres based on consumption rank [1]. Even though their properties exhibit an attractive balance of low cost, strength, modulus and chemical resistance, numerous attempts are constantly made for the improvement of their properties [2]. Improvement of the performance of polypropylene by using modifiers of nanometric granulation has been the aim of intensive research conducted in recent years in laboratories all over the world [2 - 16]. The most popular purpose of the addition of different nanoparticles into a polymer matrix is polymer reinforcement [2 - 7], the enhencement of barrier properties [3] or the improvement of conductivity [4]. Some of them also refer to fibre spinning polymer materials [2, 4, 5, 9, 10]. It should be noted that, in contrast to the countless applications of iPP plastics modified with nanoadditives, the area of melt-spun iPP fibres modified is still not developed enough. The nanoadditives that have been most intensively used for iPP fibres modification trials are nanoclays and carbon nanotubes (CNTs) [5, 6, 7].

In general the improvement of mechanical properties can be achieved through the sufficient concentration and dispergation of the nanoadditive, which facilitates the convenient aligment of nanoparticles in the polymer matrix, and through the functionalisation of the nanoparticle surface, thereby improving the formation of the interphase between components of the system [6, 8]. There are many results that indicate the real improvement of the mechanical properties of polypropylene nanocomposites as the result of nanoadditive application, but only a few show significantly improved properties of composite fibres [4, 9, 10].

The nature of nanopowders, their natural ability to agglomerate and the drastic change in rheological parameters of the melt containing them [11] causes that the mechanical parameters of most melt-spun fibres with the addition of nanomodifiers are far from satisfactory, as multiple problems appear during fibre spinning.

It was found that the combination of stretching and the addition of multi-walled carbon nanotubes (MWCNTs) can enhance the yield strength and Young's modulus of modified iPP fibres by up to 84% [10]; however the improvement depends on the concentration of nanoadditives and stretching rate [4, 9]. According to literature, a too high concentration of nanoparticles results in their agglomeration and triggers the improvement of properties. The other problem is the strong nucleation ability of MWCNTs in iPP composites [12]. Hence a lower content of the nanoadditive is more beneficial not only for material properties but also from an economical point of view.

During the last decade at the Institute of Textile Engineering and Polymer Materials, University of Bielsko-Biala, a few scientific programs have been realised dedicated to melt-spun polymer nanocomposite fibres. First of all, organo montmoryllonite clays were tested, both commercial and noncommercial [13 - 15]. Recently there have been successful trials of melt-spinning fibres with graphene and carbonnanotubes [16].
We decided to benefit from the expertise gained so far in order to obtain a spinnable polymer allowing the formation of microscopically homogeneous fibres of significantly improved tenacity.

The main goal of the modification of isotactic polypropylene (iPP) fibres with multi-walled carbon nanotubes (MWCNT) applied was either increasing the te-

nacity and enlargement of ageing resistance or the improvement of their flame-retardant properties.

The presented work is concerned with studies of the thermal properties and supermolecular structure of new composite fibres obtained from iPP – as a matrix and MWCNT used as the filler.

Within this paper we will present the results of studies carried out on composite iPP/MWCNT fibres, finally containing ca 0.2% of carbon nanotubes, formed at a take up velocity from gravity spun to 460 m/min. The fibres presented have unusually high mechanical properties, achieved through the low concentration of very well dispersed MWCNTs, which is made possible by using a two step process: the preparation of a masterbatch containing MWCNTs and application of a prototype of the spinning head. Relatively comparable results were obtained recently only by [9]; however it should be noted that they applied DR = 7 and compatibilisers. In the present case, the tenacity of iPP/MWCNT composite fibres without the addition of compatibilisers exceeds 120 cN/tex at DR = 5, which makes this case interesting in a cognitive and technological sense.

A supermolecular structure of analogeus high tenacity (above 1 GPa) polypropylene fibres modified with single wall carbon nanotubes (SWCNT) was recently proposed by [9], based on the results of TEM and 2D-SAXS. In this paper the supermolecular structure of polypropylene fibres modified with MWCNTs is discussed based on both the wide angle (WAXS) and small angle X-ray scattering methods (SAXS). Moreover the crystalline structure of iPP/MWCNT fibres as spun and after heating treatment at a temperature of 95 °C was investigated not only by WAXS but also by the differential scanning calorimetry (DSC) method. On the basis of the results obtained the influence of the MWCNT modifier on the crystallinity index of the iPP matrix of fibres studied versus the velocity of forming was evaluated.

■ **Experimental**

Materials

The isotactic polypropylene for textile applications - Tatren TI 922 (Slovnaft Petrochemicals Co., Slovakia) with an MFI of 30 g/10 min (230 °C/2.16 kg),

and a concentrate of MWCNT Plasticyl® 2001 supplied by Nanocyl (Belgium) were used. This modifier contained 20% of carbon nanotubes - Nanocyl™ NC 7000 manufactured using the chemical vapour deposition process. A preliminary masterbatch of Plasticyl® 2001 and iPP containing 2% of MWCNT was prepared using the laboratory technological line Maris TM 58 MW40 (Italy) equipped with a two-screws extruder. The final concentration of MWCNTs in the fibre-grade polymer was 0.2%.

Microfibres for structural investigations were formed from the melt at a temperature of 240 °C by means of a laboratory spinning machine at a velocity of v_0 – gravity spun, v_1 = 123.5 m/min, v_2 = 247.0 m/min, v_3 = 358.8 m/min and v_4 = 460.6 m/min, respectively.

In order to assess mechanical parameters and to explain the transformation of the supermolecular structure, fibres were subjected to drawing at 95 °C (draft ratio DR = 5) and at a drawing velocity of 0.5 m/min.

Methods

Scanning Electron Microscopy (SEM) analyses were performed in the conventional SEM mode using a Jeol JSM 5500LV (Japan) instrument operating at 10 kV after coating the samples with a thin layer of gold by sputter deposition. The surfaces of samples were observed at magnifications from ×1 000 up to ×10 000.

Tensile strength parameters of the microfibres iPP/MWCNT were defined according to the standard PN-EN-ISO 5079:1995 [17] by means of the tensile testing machine INSTRON 5544 Single Column (USA) [18]. The machine consisted of a press- stretching head for fibres of static load cell rating ±10 N, with an indication error of 0.05%. Samples of 10 mm length were conditioned at normal conditions, placed on the testing window frames and measured using the tensile testing machine [19]. The tensile speed was 40 mm/min and 50 tests were made for each sample. The measurements during which the fibre was broken directly in the grips were rejected.

The diameters of fibres were measured by using a lanameter (300 measurements, random error below 3%) and confirmed by optical and electron microscopy.

Calorimetric (DSC) investigations were carried out using a TA Instruments (USA) Thermal Analysis System 5100 equipped with a Differential Scanning Calorimeter model 2920. The linear function of temperature increase was used. The samples of fibres were heated at a rate of 10 °C/min from -60 °C to 250 °C (atmosphere N_2; flow 40 ml/min). The heat and temperatures of transitions were calculated by means of Universal V2.6D TA Instruments software.

Wide angle X-ray scattering (WAXS) investigations were carried out with a URD 63 Seifert diffractometer (Germany). CuK_α radiation was used at 40 kV and 30 mA, and a scintillation counter as a detector. Investigations were performed in the range of angles 4° to 40° with a step of 0.1°.

Small angle X-ray scattering (SAXS) investigations were performed by means of
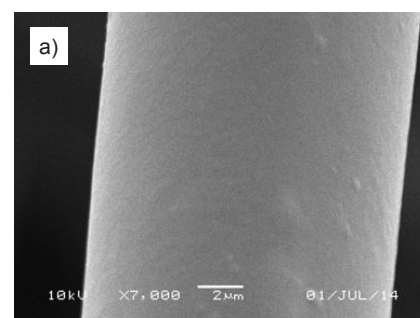
Figure 1. *SEM microphotographs of iPP/MWCNT modified undrawn (raw) v_4 microfibres, magnifications: a) ×7 000.*
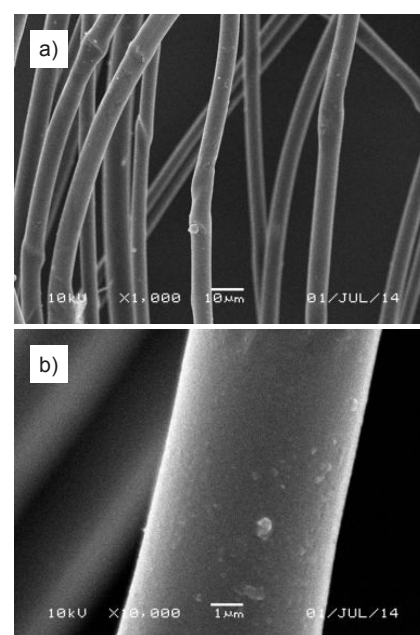
Figure 2. *SEM microphotographs of iPP/MWCNT modified drawn microfibres v_{4R}, magnifications: (a) ×1000; (b) ×10 000.*

Table 1. Mechanical parameters, for undrawn microfibres iPP/MWCNT.

Sample	Force, cN	Breaking tenacity, cN/tex	Breaking tenacity, MPa	CV$_T$, %	Elongation at break, %	CV$_E$, %
v$_1$	4.12	25.74	230.1	15	242	57
v$_2$	3.50	39.75	355.3	17	216	49
v$_3$	0.94	18.10	161.8	20	197	77
v$_4$	0.60	37.10	331.6	29	126	56

Table 2. Mechanical parameters, for drawn microfibres iPP/MWCNT.

Sample	Force, cN	Breaking tenacity, cN/tex	Breaking tenacity, MPa	CVT, %	Elongation at break, %	CV$_E$, %
v$_{1R}$	3.74	74.26	663.8	41	86	67
v$_{2R}$	3.60	121.75	1088.2	20	20	54
v$_{3R}$	1.57	91.28	815.8	46	23	54
v$_{4R}$	1.38	112.51	1005.6	38	19	48

a MBraun camera (Austria), which utilises conventional Kratky collimation system. The front of the camera was directly mounted on the top of the tube shield of a stabilised Philips PW 1830 X-ray generator (the Nederlands). The X-ray tube was operated at a power of 1.5 kW, and CuK_α radiation was used. Scattered radiation was recorded in an acquisition time of 900 s by means of a MBraun linear position-sensitive detector, model PSD 50. The detector had 1024 channels with a channel-to-channel distance of 52 µm.

■ Results and discussion

SEM micrography

The thicknesses and shapes of the iPP/MWCNT modified fibres are regular and the surfaces smooth and plain (*Figure 1* and *Figure 2.a*, & *2.b*), as the low concentration (0.2%) of modifying carbon nanotubes allows to prevent agglomeration of the additives. As a result of drawing, one can observe a decrease in fibre diameters as compared to undrawn fibres (*Figure 1, Figure 2.b*).

Mechanical tests

Based on the mechanical measurements, we defined the average breaking tenacities of the microfibres, relative elongation at break and corresponding coefficients of variation.

Average tensile test results are collected in *Tables 1* and *2*. Stress-strain curves characteristic for fibres spun at a velocity of v_2 (before drawing) are presented in *Figure 3*, and for drawn fibres in *Figure 4*. The dispersion of results of the breaking force and breaking elongation was relatively high in both cases, as can be seen in *Figures 3* and *4*. The coeffi-

cient of variation for the breaking tenacity was in the range of 15 – 30% in the case of undrawn fibres, and in the range of 20 – 50% for drawn fibres. Along with the increase in spinning velocity, that in the breaking tenacity and decrease in the elongation at break was noticed both for undrawn and drawn fibres (*Tables 1 & 2*). Moreover it should be noted that average values of strain for fibres formed at the same spinning velocity increase after drawing, while those of elongation decrease, respectively.

In dependence on the spinning velocity, the diameters of MWCNT modified microfibres before drawing were in the range of 4 – 16 µm, and after drawing in the range of 2 – 8 µm. The number of fault measurements (fibres broken during setting in the clamps) was at the level of 20 – 40% for fibres before drawing and slightly higer for drawn fibres (30 – 50%). Only correct measurements were taken into account, which means when fibre breakage was noticed roughly in the middle of its length.

In general it can be stated that the results of mechanical tests of iPP/MWCNT microfibres confirm the regularity observed in most cases of microfibres, that is the stiffness and tenacity of microfibres subjected to drawing is significantly higher as compared to undrawn microfibres.

There should be special attention paid to the very important fact that iPP/MWCNT fibres exhibit significantly higher tenaci-
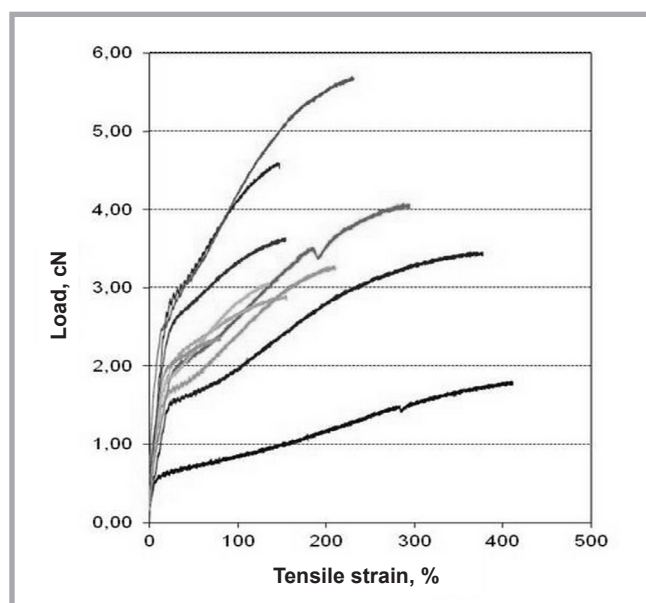
Figure 3. Exemplary diagram of stress-strain curves of undrawn microfibres iPP/MWCNT for v_2.
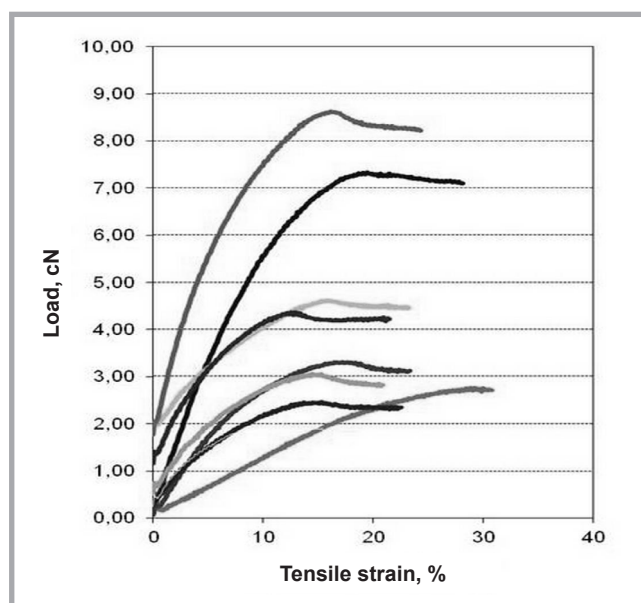
Figure 4. Exemplary diagram of stress-strain curves of drawn microfibres iPP/MWCNT for v_{2R}.

ties as a result of drawing (*Figure 3*). For example, in the case of fibres spun at the velocity $v_2 = 240$ m/min, the tenacity after drawing is four times higher as compared to classic textile polypropylene fibres [20].

DSC investigations

It is worth presenting calorimetric results starting from q comparison of DSC curves of iPP/MWCNT and pure iPP during nonisothermal crystallization from melt (*Figure 6*). In the case of material containing carbon nanotubes (*Figure 6* curve b), the exothermic peak of crystallisation is shifted towards higher temperatures. The so-called extrapolated beginning of crystallisation, corresponding to the temperature of the nucleation, is 3.4 °C higher in the case of iPP/MWCNT as compared to pure iPP. This is clearly evidence of MWCNT presence in the material, acting upon the heterogeneous nucleants. Moreover the different shape of the peak of crystallisation in the case of iPP/MWCNT and the higher value of enthalpy of crystallisation ΔH_m (ca 7 J/g), as compared to iPP, indicate the effect of the presence of carbon nanotubes on the kinetics of nonisothermal crystallisation of the system.

Simultaneously in the DSC part of our study it was interesting to define the influence of the take up velocity of iPP/MWCNT microfibres on their nanostructure order level.

In the case of undrawn microfibres, all registered DSC curves, irrespective of the speed of formation, have the same character (*Figure 7*, curve – a, see page 42), revealing analogical thermal effects – recrystallisation and melting. Values of the characteristic temperatures and enthalpies of recrystallization and melting: T_r, T_m, ΔH_r, ΔH_m, respectively, evaluated on the basis of DSC curves are shown in *Table 3*.

It is worth noticing that the value of the minimum temperature of the melting peak in relation to the fastest melting of crystallites does not change considerably for all fibres studied, which may indicate that an increase in the take-up velocity changes the content of the crystalline fraction in the modified iPP/MWCNT microfibres without causing a distinct change in the mean size of crystallites.

In the case of microfibres drawn at 95°C, for all variants of spinning velocity, the endothermic effect of recrystallisation on
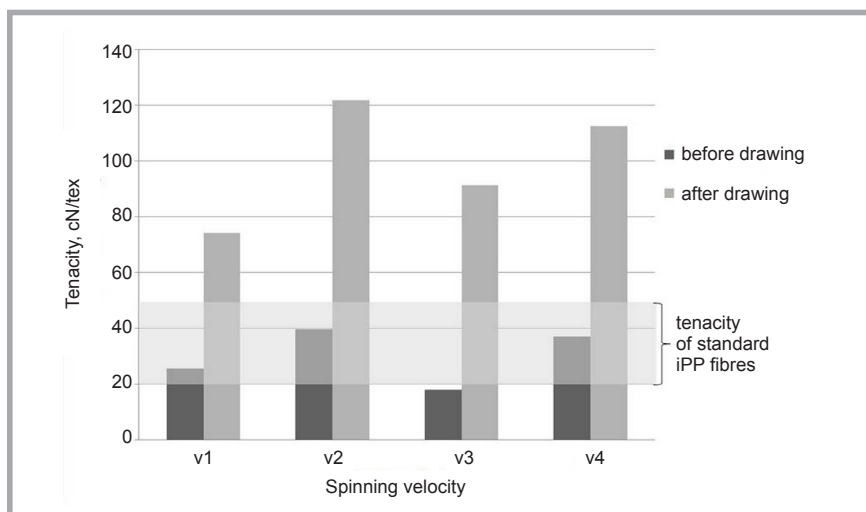

Figure 5. Breaking tenacity of iPP/MWCNT microfibres spun at spinning velocities of $v_1 – v_4$.

Table 3. Values of temperatures of recrystallisation Tr & melting Tm, and enthalpies ΔHr & ΔHm, respectively for undrawn iPP/MWCNT microfibres formed at a different take-up velocity.

Sample	Temp. of recryst. T_r, °C	Enthalpy of recryst. ΔH_r, J/g	Temp. of melting T_m, °C	Enthalpy of melting ΔH_m, J/g
v_1	107.1	14.40	164.0	88.97
v_2	106.2	14.46	164.8	94.51
v_3	120.9	17.10	164.0	95.81
v_4	116.7	18.70	164.0	100.10

Table 4. Values of temperatures of recrystallisation T & melting Tm, (temperatures of additional melting peak in brackets) and enthalpies ΔHr & ΔHm, respectively for drawn iPP/MWCNT microfibres formed at a different take-up velocity.

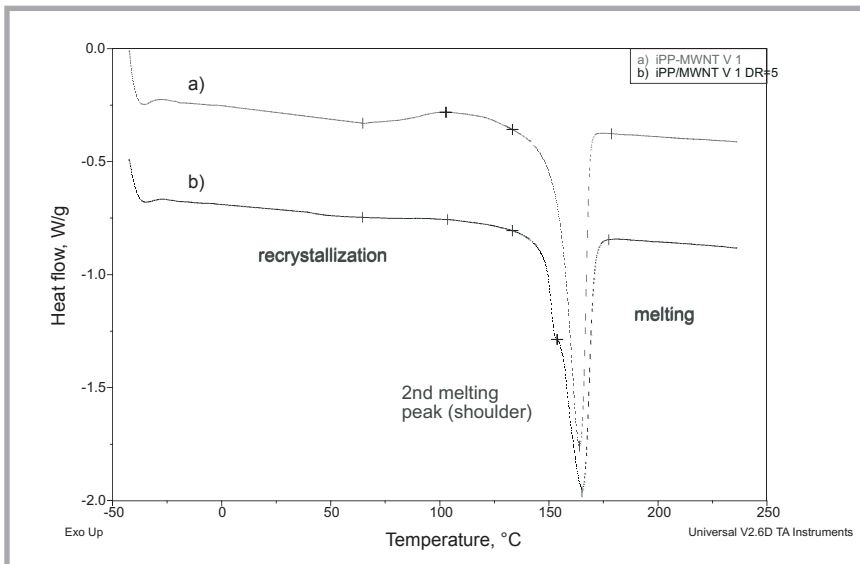| Sample	Temp. of recryst. T_r, °C	Enthalpy of recryst. ΔH_r, J/g	Temp. of melting T_m, °C	Enthalpy of melting ΔH_m, J/g
v_{1R}	103.5	2.89	(153.0) / 165.2	93.49
v_{2R}	109.6	2.89	(157.9) / 166.5	102.90
v_{3R}	105.5	3.88	(159.4) / 166.5	103.20
v_{4R}	111.2	2.82	(159.7) / 166.9	96.54
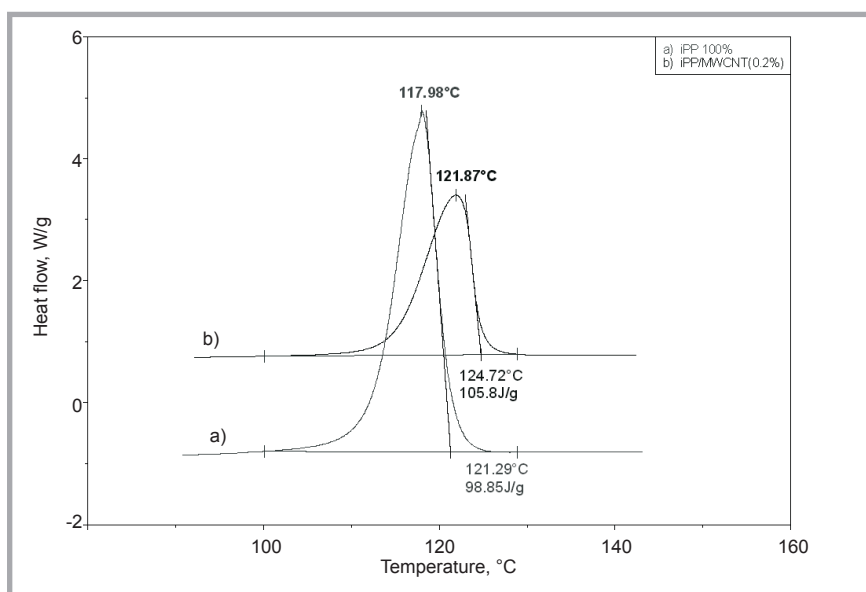
Figure 6. DSC curves registered during control cooling (10 °/min) from melt for the pure iPP (curve – a) and iPP/MWCNT (curve – b), respectively.

Figure 7. DSC curves registered during heating for the iPP/MWCNT microfibres investigated, formed at a velocity of v1 before (curve – a) and after the drawing process (curve – b).

DSC curves practically disappears, while values of the enthalpy of melting clearly increase, as expected, wherein the peak of melting is clearly bimodal (***Figure 7***, curve – b). The reason for the effects observed is the recrystallisation of the fibre material taking place during thermal treatment accompanying the drawing. According to the data from X-ray diffraction experiments, the recrystallisation refers to the transformation of the smectic most of all– the mesomorphic phase of microfibres to a thermodynamically stable α-iPP crystalline form.

Analogous to undrawn microfibres, values of the characteristic temperatures and enthalpies: T_r, T_m, ΔH_r, ΔH_m, respectively, for iPP/MWCNT fibres after process of drawing are shown in ***Table 4*** (see page 41).

Diffraction study

Figure 8 presents a comparison of WAXS curves of raw and drawn iPP/MWCNT microfibres formed at a velocity of v_1. The WAXS patterns shown in this figure contain characteristic reflections of (110), (040) and (130) planes of α-form crystals of isotactic polypropylene. The curve of raw fibres also contains an additional maximum at $2\Theta \approx 15°$, indicating that a special type of order-mesophase exists in the supermolecular structure of the microfibres.

The supermolecular structure of microfibres formed during the spinning is the result of the processes of orientation and crystallization occurring by solidifying the polymer stream. During the formation of a fibre, the process of crystallisa-

tion occurs under non-isothermal conditions and different types of flow fields (shear, extension, mixed). Furthermore, the addition of carbon nanotubes into sheared polymer melts complicates the crystallisation process. As a result of these processes, a structure comprising of three phases is formed.

In order to look more closely at the proportion of these particular phases, namely the amorphous , mesophase and crystalline phases, WAXS curves were deconvoluted into individual peaks using the profile fitting program WaxsFit [21]. Each peak was modelled using a Gaussian-Cauchy peak shape. The content of the crystalline α-form of polypropylene, x_α, was calculated as a ratio of the area under the crystalline peaks, corresponding to that phase, to the total area of the scattering curve. Similarly the content of mesophase, x_m, was determined as a ratio of the area under the mesophase peak at $2\Theta \approx 15°$ to the total area of the scattering curve. The overall crystallinity index $x_c = x_\alpha + x_m$. ***Figure 9***, is a representative example of a diffraction curve that has been resolved into individual scattering components using peak fitting software. Results are presented in ***Tables 5*** and ***6***.

To evaluate variations in the crystallite sizes of iPP, the Scherrer equation was used. Crystallite sizes were calculated in the direction perpendicular to the (110), (040) and (130) planes. The content of the meso- and crystalline phases varies depending on the take-up velocity. At a take-up velocity of 460 m/min the mesophase content achieves a maximum value. The crystallite sizes of raw microfibres change in the range 11.4 – 19.2 nm
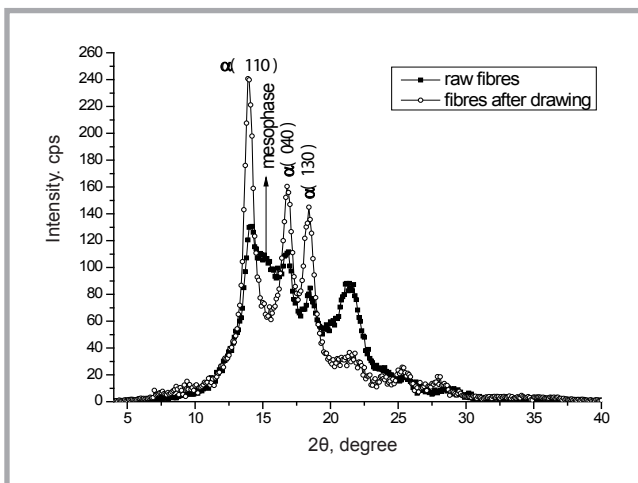
Figure 8. *Comparison of WAXS curves for raw and drawn v_1 microfibres.*
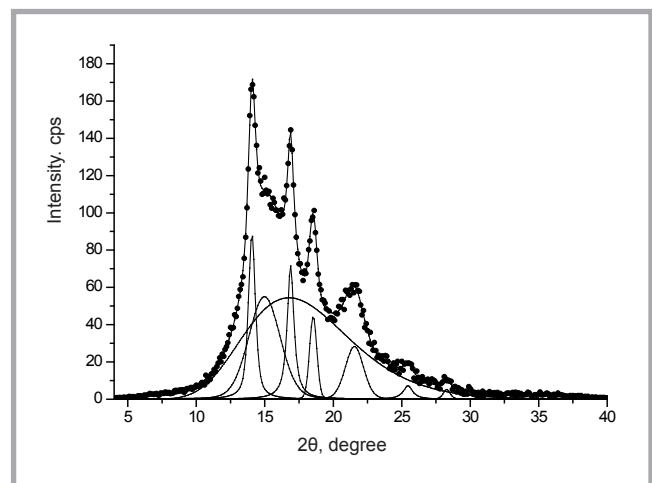

Figure 9. *WAXS curve resolved into individual peaks for raw v_1 microfibres.*

and slightly decrease after the drawing of fibres. Irrespective of the take-up velocity for raw fibres, values of the long period are almost the same and equal to approximately 10.5 nm. The values of the crystalline and amorphous layer thicknesses are equal to 3.0 nm and 7.5 nm, respectively. After drawing, the crystal layer thickness l_C remains practically constant. Hence changes in the long period L are caused only by an increase in the amorphous thickness l_A. Stretching the fibres does not cause deformation of the lamellar system generally, since the stresses are carried by the disordered interfibrillar regions [22]. It appears that for the fibres tested containing carbon nanotubes, the mechanism is partially blocked by the presence of nanotubes in the interfibrillar areas of these fibres.

Figure 10 shows SAXS curves taken in the direction parallel to the fibre axis for raw and drawn v_2 microfibres. This figure represents SAXS profiles plotted against the scattering vector s, given by $s = (2/\lambda)\sin(\theta/2)$, where λ and θ are the wavelength of the X-ray and the scattering angle, respectively. Both SAXS profiles show a discrete maximum, which is connected with the lamellar structure of polypropylene. The SAXS peak intensity increases significantly, and its angular position shifts to lower s values, which corresponds to larger long spacings of the lamellar stacks. Detailed characterisation of the lamellar structure of the polypropylene matrix in composite microfibres was performed by means of the one-dimensional correlation function, which was derived from SAXS curves by Fourier transformation. This function allows for determination of values of the long period L as well as crystalline and amorphous layer thicknesses l_C and l_A, respectively [23]. Results are presented in ***Table 7***.

Conclusions

Based on the results presented, it can be stated that the method applied to prepare spinnable isotactic polypropylene modified in a melt state by the addition of carbon nanotubes, at a concentration of 0.2%, and adopting conditions of mixing, spinning and stretching, turned out to be correct and very promising. Homogeneous iPP/MWCNT microfibres were obtained in a wide range of spinning velocities up to 460 m/min. In the case of fibres spun at spinning velocity
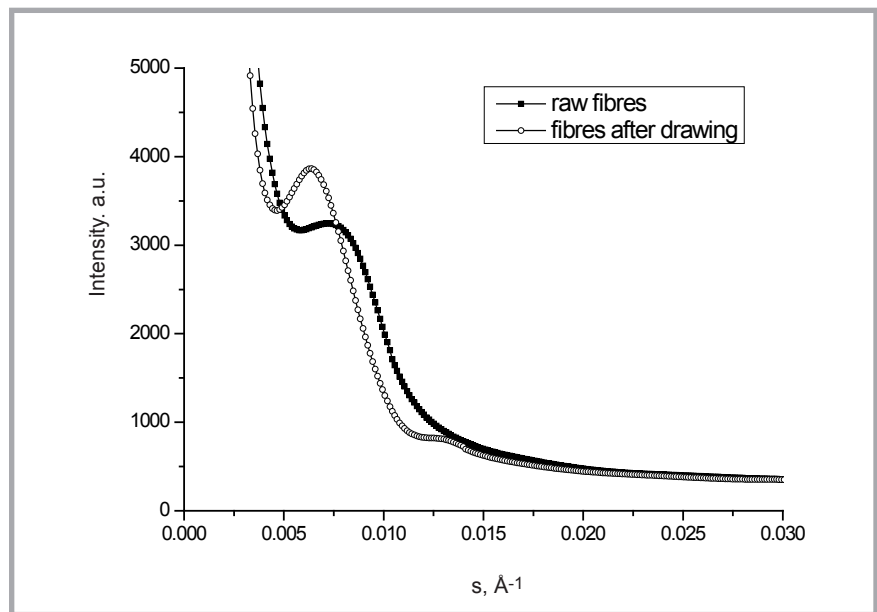
Figure 10. *Comparison of SAXS curves for raw and drawn v_1 microfibres.*

Table 5. *Results of WAXS measurements for raw iPP/MWCNT microfibres.*

Sample	Overall crystallinity x_c, -	Content of α form $x_α$, -	Content of mesophase x_m, -	Sizes of crystallites of α-iPP form, nm			Sizes of mesophase crystallites, nm
				$D_{(110)}$	$D_{(040)}$	$D_{(130)}$	
v_0	0.546	0.546	–	18.3	19.2	13.5	-
v_1	0.370	0.221	0.149	11.7	13.1	14.6	3.1
v_2	0.399	0.254	0.142	12.7	14.6	11.4	3.3
v_3	0.418	0.269	0.149	15.0	14.0	12.6	3.4
v_4	0.427	0.248	0.179	14.5	15.2	14.2	2.7

Table 6. *Results of WAXS measurements for iPP/MWCNT microfibres after drawing.*

Sample	Overall crystallinity x_c, -	Sizes of crystallites of α-iPP form, nm		
		$D_{(110)}$	$D_{(040)}$	$D_{(130)}$
v_{1R}	0.516	12.3	11.3	10.5
v_{2R}	0.508	10.6	10.7	10.0
v_{3R}	0.467	12.0	12.0	10.5
v_{4R}	0.440	12.0	12.2	11.0

Table 7. *Results of SAXS measurements for raw and stretched fibres containing a long period L and crystalline and amorphous layer thicknesses: l_C and l_A, respectively.*

Sample	Long period L, nm	Thickness of crystalline layers l_C, nm	Thickness of amorphous layers l_A, nm
v_1	10.3	2.68	7.62
v_2	10.6	3.02	7.58
v_{1R}	11.4	2.94	8.46
v_{2R}	12.3	3.39	8.91

$v_2 = 247.0$ m/min and subsequently drawn at $DR = 5$ the average tensile strength exceeded a value of 120 cN/tex, not recorded so far in literature. Based on high values of the tensile strength, we concluded there was proper dispersion of MWCNT within the iPP matrix. However relatively high values of CV are most probably the result of the drawback of spinning line such as weak balance of the winder and not perfect stability of drawing.

The Research presented indicates that the supermolecular structure of iPP/MWCNT microfibres is analogous to the structure of classical fibres melt-spun from semicrystalline thermoplastic polymers. It is possible to identify fibrils (fibril aggregates) containing so-called stacks of crystalline lamella. However, it is pecu-

liar that in the case of undrawn microfibres, the lack of a complete crystalline arrangement was observed for some lamella. This resulted in a mesomorphic smectic phase identified in both WAXS patterns in the form of the widening of crystalline maxima, as well as on DSC curves in the form of small recrystallisation exotherm. As a result of the drawing process at a temperature of 95 °C, the effects discussed above disappear. The smectic phase of polypropylene transforms into the more thermodynamically stable α-iPP structure. Such a phenomenon used to be observed in the case of unmodified polypropylene fibres, but spun at much higher spinning velocities, that is above 2.500 m/min [24].

The scattering patterns of undrawn iPP/MWCNT microfibres in the range of small angle X-ray scattering, described by the long period L, basically do not differ from the values obtained for conventional iPP fibres. A substantial difference (as compared to iPP fibres modified with nanoclays [22]) was noticed during the structure transformation accompanying the drawing process. In the case of iPP/MWCNT microfibres, a pronounced increase in long period values is observed with increasing deformation, macroscopically demonstrated as fibre elongation. This results from an increase in the size of amorphous interlamellar spacing of the lamellar stacks. Consequently this allowed the hypothesis that carbon nanotubes are located in interfibrillar spaces of the microfibres, causing the tacking of adjacent fibrils and, particularly, a reduction in their mobility during the deformation accompanying drawing.

The above conception is quite a convincing explanation for the very substantial increase in tensile strength of the iPP/MWCNT after drawing.

References

1. Yang Qin M. Global Fibres Overview. In: *Synthetic Fibres Raw Materials Committee Meeting at APIC 2014*, Pattaya, 16 May, 2014.
2. Rault F, Campagne Ch, Rochery M, Giraud S, Devaux E. *Journal of Polymer Science Part B: Polymer Physics* 2010; 11: 1185–1195.
3. Sanchez-Garcia MD, Lopez-Rubio A, Lagaron JM. *Trends in Food Science & Technology* 2010; 21: 528–536.
4. Marcincin A, Hricova M, Ujhelyiova A. IOP Conf. Series: *Materials Science and Engineering* 2014; 64: 012004.
5. Marcinčin A, Hricová M, Marcinčin K, Hoferíková A. *Fibres & Textiles in Eastern Europe* 2009; 17, 6(77): 22–28.
6. Spitalsky Z, Tasis D, Papagelis K, Galiotis C. *Progress in Polymer Science* 2010; 35: 357.
7. D. Bikiaris, A. Vassiliou, K. Chrissafis, K.M. Paraskevopoulos, A. Jannakoudakis, A. Docoslis. *Polymer Degradation and Stability* 2008; 93: 952.
8. Moll JF, Akcora P, Rungta A, Gong S, Colby RH, Benicewicz BC, et al. *Macromolecules* 2011; 44(18): 7473-7477.
9. Gao Y, Zong G, Bai H, Fu Q. *Chinese Journal of Polymer Science* 2014; 2: 245–254.
10. Soitong T, Pumchusak J. *Journal of Materials Science* 2011; 46: 1697–1704.
11. Krishnamoorti R, Vaia RA. *Journal of Polymer Science Part B: Polymer Physics* 2007; 24: 3252–3256.
12. Assouline E, Lustiger A, Barber AH, Cooper CA, Klein E, Wachtel E, Wagner HD. *Journal of Polymer Science Part B: Polymer Physics* 2003; 5: 520–527.
13. Ślusarczyk Cz, Biniaś W, Fabia J, Biniaś D. *Fibres & Textiles in Eastern Europe* 2007; 15, 5–6(64–65): 22.
14. Ślusarczyk Cz, Janicki J, Fabia J. *Polish Journal of Applied Chemistry* 2011; 55, 3–4: 97.
15. Brzozowska-Stanuch A, Rabiej S, Fabia J, Nowak J. *Polimery* 2014; 59, 4: 302.
16. Fryczkowski R, Gorczowska M, Ślusarczyk Cz, Fryczkowska B, Janicki J. *Composites Science and Technology* 2013; 80: 87.
17. Textiles – Fibres – Determination of breaking force and elongation at break of individual fibres. ISO 5079: 1995.
18. Technical-motion documentation of a resistance machine INSTRON – model 5544.
19. Textiles – Standard atmospheres for conditioning and testing. ISO 139:1973.
20. Włodarski G. *Włókna chemiczne. Pradnik inżyniera i technika*. Ed. WNT, Warsaw 1977.
21. Rabiej M. *Polimery* 2003; 48: 288.
22. Ślusarczyk Cz. *Journal of Alloys and Compounds* 2004; 382: 68.
23. Ślusarczyk Cz, Fabia J, Janicki J, Bączek M. SAXS characrerization of structural changes in polyamide 6/montmorillonite nanocomposite fibers during annealing and drawing. In: *XIV International Conference on Small-Angle Scattering SAS 2009*. Oxford, England, September 13–18, 2009.
24. Fabia J. *Struktura nadcząsteczkowa włókien polipropylenowych modyfikowanych elastomerami*. Doctoral thesis, Akademia Techniczno-Humanistyczna, Bielsko-Biała, 2001.

15th Autex World Textile Conference, AUTEX 2015

10 - 12.06.2015, Bucharest, Romania

The Conference will focus on the most relevant topics and issues of European and global science in the field of textile materials, technologies, fashion, design, management and marketing.

Conference topics:
- Advanced fibres and materials
- Smart, functional and interactive textiles
- Biopolymers and biotechnology
- Medical textiles, tissue engineering
- Nanotechnology, nanotextiles, electrospinning
- Finishing, dyeing, surface functionalization and coating
- Textile processing (spinning, weaving, knitting, nonwoven, braiding)
- Textile testing, measuring technology
- Textile and clothing equipments
- Quality control systems and devices in textiles and clothing
- Fashion and design in textile industry
- Textile economy, textile supply chain management
- Comfort science
- Life cycle assessment in textiles
- Sustainable textile processes
- Modeling and simulation in textiles
- Textile membranes
- CAE technologies and mass customization
- Textile based composites
- Textile education and training
- Technical and protective textiles
- 2B FUNTEX themes: innovative functional textiles
- Sustainable innovation for leather and footwear industry

Chairperson of the Scientific Committee:

Maria Carmen Loghin, The Gheorghe Asachi Technical University of Iaşi, Romania

The Scientific Committee consists of 42 outstanding scientists from around the world.

Chairperson of the Organizing Committee:

Mirela Blaga, The Gheorghe Asachi Technical University of Iaşi, Romania

For further information:
http://www.autex2015.ro